International Research Journal of Engineering and Technology (IRJET) e-ISSN: 2395-0056
Volume: 05 Issue: 05 | May-2018 www.irjet.net p-ISSN: 2395-0072

Design of Photonic Quasi Fiber for the Generation of Polarization Maintaining Super-continuum using Ellipticity Concept

Narmathashri.P[1], Grace Shoba.S.J[2]

[1]ME-Applied Electronics, Department of Electronic and Communication Engineering, Velammal Engineering College Chennai-600066, India.
[2]Professor , Department of Electronic and Communication Engineering, Velammal Engineering College Chennai-600066, India.

Abstract - *A chalcogenide $Ge_{11.5}As_{24}Se_{64.5}$, photonic quasi-crystal fiber for broadband mid-IR supercontinuum generation (SC) has been reported. The numerical demonstration of SC generation in the proposed PQF spans from 2 to 15 µm wavelengths for a pulse power of 2 kW. Besides, the proposed PQF offers a high birefringence (10^{-3} to 10-2) from 3.5 to 15 µm wavelengths and exhibits a low confinement loss ($10^{-7}$to 10^{-1}) for the wavelengths from 2 to 15 µm with single mode behavior. The proposed $Ge_{11.5}As_{24}Se_{64.5}$ photonic quasi crystal fiber is designed with zero dispersion wavelength at 4.33 and 4.46 µm for x and y polarized modes within the wavelength range of 2-15 µm. Hence, the orthogonally polarized modes allow the high degree of freedom in the tuning the properties of super continuum. The polarized spectral broadening of continuum is realized for the first time from 2 to 15 µm using the proposed PQF with a length of 8 mm. Thus, the proposed PQF based SC source is a good candidate for applications such as optical communication, early cancer diagnostics, optical sensing, optical tomography and frequency metrology.*

***Key Words*: Non-linear optics, Photonic Quasi-Crystal fiber, Super continuum generation**

1.INTRODUCTION

Ultra-broadband SC sources have demand in various applications from material processing to medical [1, 2, 3]. In particular, the broadening of the SC spectrum greatly depends on the structural and the pump pulse parameters as well as material properties of the medium. The quality of the SC is greatly improved by controlling the non-linearity, group velocity dispersion (GVD), CL and birefringence of the optical fiber. These properties are extensively engineered by micro-structured optical fibers (MOFs), which have been considered as a dominant medium in supercontinuum generation (SCG). Unfortunately, the use of silica MOFs in the infrared wavelengths above 2.5 µm are limited by high material absorption [3]. Hence, the attention has turned to non-silica MOFs that include tellurite, fluoride and chalcogenide (ChG) glasses. These superior properties of ChGs are utilized to generate wideband SC in MIR.

To date, the variety of ChG glass MOFs such as photonic crystal fiber [4], photonic bandgap fiber [5], microporous fiber [6], suspended core fiber [7] and large mode area (LMA) fiber [8] have been analysed theoretically and experimentally in order to tailor the linear and non-linear properties to enhance the SCG. Recently, Cheng et al have fabricated $AsSe_2As_2S_5$ (core-clad) hybrid MOF which was pumped with three different wavelengths of 3.062, 3.241 and 3.389 µm for SCG from 1.256 to 5.400 µm [9]. Further, Kubat et al. have numerically modeled the MIR-SCG in the three wavelength ranges of 12.5 µm, 10.7 µm and 10.6 µm in the As-Se/GeAsSe (core/clad) fiber with core diameter of 8, 10 and 20 µm at the length of 2m and 3m, respectively [10]. Besides, Tang et al. have proven the possibility to achieve a low loss in GeAsSe fiber (0.083 dB/m) at a wavelength of 6.6 µm [11]. Very recently, Yu et al. have reported the experimental results on SC spanning from 1.8 to 10 µm by pumping at 4 µm wavelength in a small core GeAsSe/GeAsS (core/clad) fiber with a length of 11 cm [12]. Among the various MOFs, we prefer the six-fold symmetry PQF due to its single mode maintaining characteristics up to an air-filling ratio of 0.525. In the recent past, the PQFs have been used widely to tune the fiber characteristics such as single mode behaviour [13], large mode area [14], birefringence [15], dispersion [16] and non-linearity [17]. Besides GVD and non-linearity, the polarization is also an essential characteristic in the dynamics of SCG in mid IR region. Generally, a high birefringence can be achieved in the MOF by following any one of the structural variations such as elliptical air holes, holes with liquids and non-uniform air holes. On the contrary, extending a high birefringence and a low CL beyond 10 µm wavelength is restricted in the PQF by means of an air-filling fraction. The maximum value of air-filling ratio to maintain the single mode nature in PQF is 0.44 [18]. This value restricts the increase of the air hole size which in turn results in high losses for fundamental mode (FM) in longer wavelengths.

In this paper, we propose numerical demonstration of GeAsSe PQF for MIR SCG. We utilize the unique characteristics of PQF (V number =π for the air-filling ratio of 0.525) [19] which offers a great flexibility in increasing the air hole size without compromising the single mode nature of the fiber. Further, we exploited the high transparency of $Ge_{11.5}As_{24}Se_{64.5}$ ChG glass in the mid-band region of IR (2-15 µm). Besides, the optimized low loss PM PQF shows ZDWs at 4.33 and 4.46 µm for X and Y polarized modes with a non-linearity of 0.2 W^{-1} m^{-1}. These characteristics of the proposed PQF can act as a promising candidate for polarization

preserved SCG in MIR region. Furthermore, the numerical demonstration of the SCG for a low peak power of 2 kW at pump wavelength of 4.1 μm results in a broad continuum from 2 to 15 μm wavelengths in the proposed fiber for the length of 8 mm

2. DESIGN OF THE PROPOSED PQF

In this section, we discuss the design of the proposed low loss PM PQF for SCG. Fig. 1 shows the cross sectional view of the proposed PQF. The fiber consists of air holes with two different diameters that are distributed in the $Ge_{11.5}$ $As_{24}Se_{64.5}$ background. The arrangement of air holes follow the six fold symmetry with four rings of PQF structure. The air hole to air hole spacing is denoted as pitch, λ and fixed as 8 μm, since, below this value the field does not confine into the core. On the other hand, when λ exceeds 8 μm, the CL increases and concurrently, birefringence gets reduced. This structure has two large air holes in the first ring with a diameter of d_L, varies from 6.4 to 6.6 μm. The lower limit of d_L is determined based on the previous study on high birefringence [19]. On the other hand, the upper limit of d_L is fixed such that the merging of adjacent air holes during the fabrication can be avoided.

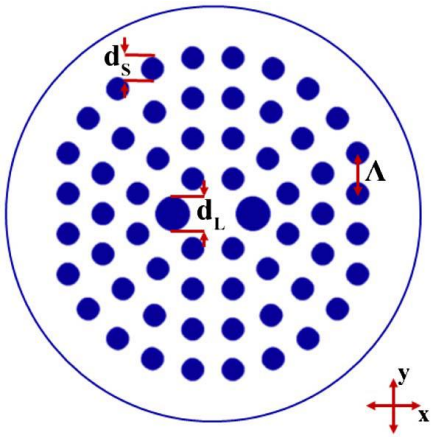

Fig -1: Cross section of proposed PM PQF. White back-ground and blue circle signifies $Ge_{11.5}$ $As_{24}Se_{64.5}$ glass and air holes, respectively.

3. MODAL CHARACTERISTICS OF PROPOSED PQF

In this section, as a first step, we calculate the effective index of FM for the proposed PQF by using the full vectorial finite element method (FEM). This effective index is an elementary parameter to estimate the linear properties such as CL, birefringence, group velocity dispersion (GVD) and higher order dispersions (HODs).

3.1 Confinement loss and birefringence

In this sub-section, we optimize the air hole diameters of d_S and d_L in order to achieve the low CL and the high birefringence, respectively.

Fig.2 shows the CL of FM as a function of wavelengths when $d_S = d_L$ = 3.8 μm and 4.2 μm for X and Y polarization modes. From the figure, it is very clear that the CL gets decreased while the diameter of the air hole, d_S is increased. In addition, the CL increases when the wavelength increases. In particular, the CL is maintained lesser than 0.1 dB/m and 0.05 dB/m when diameter of the air holes are 3.8 μm and 4.2 μm, respectively, for all the wavelengths from 2 to 15 μm. According to report on [20], single mode behaviour is found to be $V_{PCF} < \pi$ for air filling ratio of 0.44. This criteria restrict the extending of air hole diameter in PCF. At the same time, six-fold symmetry PQF explore that $V_{PQF} < \pi$ is obtained up to the air filling ratio of 0.525. This lime-lighting property of PQF offers the high degree of freedom to vary the air hole diameter of d_S from 3.8 to 4.8 μm for fixed λ of 8 μm in order to achieve d_S/λ ratio variation from 0.475 to 0.525 to sustain the single mode behavior. Hence, the maximum limit of d_S exceeds 4.2 μm, d_S/λ ratio is increased above 0.525 that has disturb the single mode behavior in the proposed PQF. Therefore, we fix the proposed PQF with the diameter of the air hole (d_S) as 4.2 μm (i.e: to achieve the maximum limit of air filling fraction of 0.525 to sustain the single mode behavior in the proposed PQF), since, it greatly exhibits a low CL without disturbing single mode nature for the wide wavelength region from 2 to 15 μm. Generally, the 6-fold symmetry PQF possesses very low birefringence (10^{-7}) due to the absence of asymmetric core structure.

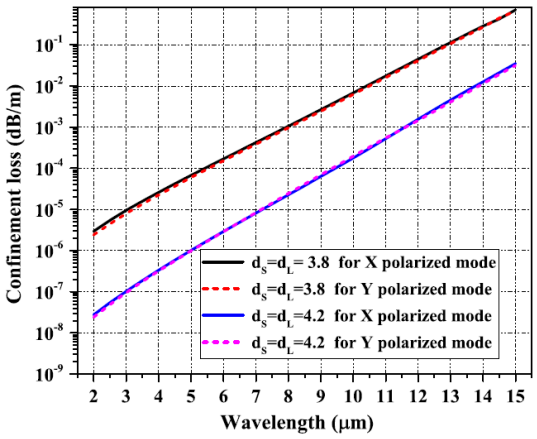

Fig -2: Variation of confinement loss against wavelengths when $d_S = d_L$ = 3.8 μm and 4.2 μm for X and Y polarized modes.

Fig. 3 shows the variation of phase and group birefringence as a function of wavelengths for two different diameters of d_L such as 6.4 and 6.6 μm. From Fig. 3, it can be seen that the birefringence gets increased when the wavelength is increased. This is because of the increment in the difference between the effective indexes of two orthogonally polarized modes. Further, the increase in large air hole diameter, d_L eventually increases the birefringence because of the change of core structure from symmetric to asymmetric. When d_L is fixed as 6.4 μm, the proposed ChG PQF exhibits the birefringence in the range from $1.8 * 10^{-4}$ to $7.4 * 10^{-2}$ for the

wavelengths from 2 to 15 μm. On the other hand, when d_L is increased to 6.6 μm, the birefringence gets increased in the order of 2.46 * 10^{-4} to 9.86 * 10^{-2} for the wavelengths from 2 to 15 μm. Amongst the two d_L values, we fix 6.6 μm, since, it reinforces the high birefringence for a broad wavelength region from 2 to 15 μm. Furthermore, the beat length of $Ge_{11.5}As_{24}Se_{64.5}$ PQF varies in the range of 8 mm to 0.1 mm for 2 to 15 μm wavelengths

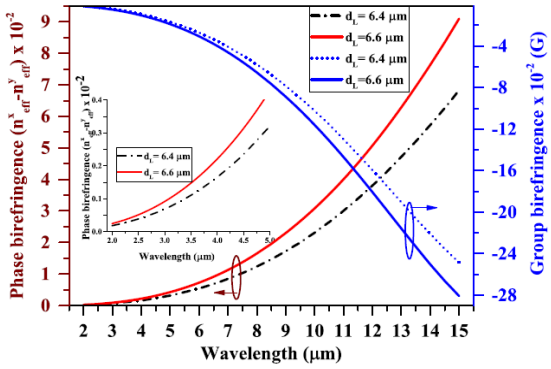

Fig -3: Variation of phase birefringence and group birefringence against wavelengths for d_L = 6.4 μm and 6.6 μm when d_S =4.2 μm. Inset, variation of phase birefringence for a wavelength range of 2 to 15 μm.

3.2 Calculation of birefringence using electrical field distribution

The proposed PQF is highly birefringent, the need for a polarizer in the output of the PQF based SC source is not required while the pump polarization is aligned along any one of the principal axes. Moreover, the preserved polarization in the proposed PQF improves the nonlinear interactions, hence, the power required to generate the SC is very minimal. In addition to, the proposed Photonic quasi crystal fiber can generate two continuum simultaneously with orthogonal polarizations which allows an additional degree of freedom to tune the properties of the Super continuum. Hence, the results of Fig. 4 confirm that the proposed $Ge_{11.5}As_{24}Se_{64.5}$ PQF has prominent PM characteristics for SC generation in the wide wavelength range from 2 to 15 μm at dL = 6.6 μm. Figure 4. (a) (b) shows the electric field distribution for X and Y polarized FMs of the proposed $Ge_{11.5}As_{24}Se_{64.5}$ PQF in the wavelengths of 4.1 and 15 μm, respectively. Figure 4 represent the field confinement of FM for X and Y polarized modes with a high B value of 2.14 × 10−3 at a wavelength of 4.1 μm. Subsequently, Figs. 4 (c) and (d) depict the field confinement of FM for X and Y polarized modes with an ultra-high B value of 9.86 × 10−2 at a wavelength of 15 μm.

3.3 Dispersion

In this sub-section, we study the dispersion characteristics of the proposed PM PQF. The variation of dispersion against wavelengths for both fast and slow axes of the proposed PM PQF is shown in Fig. 5. One can observe that the dispersion value for both fast and slow axis has the same value of -2.836 (ps/Km.nm) when the wavelength is 4.1 μm Moreover, the ZDW of the slow and fast principle axes modes are observed at 4.33 and 4.46 μm, respectively. Hence, we have selected the source pump wavelength at 4.1 μm in order to realize a wide-band parametric spectrum. From the Fig. 5, it is clear that the fast axis mode possesses the high anomalous dispersion values compared to slow axis mode beyond the wavelength of 8 μm. This is because of large second derivative of the effective index of the fast axis mode up to the wavelength of 15 μm.

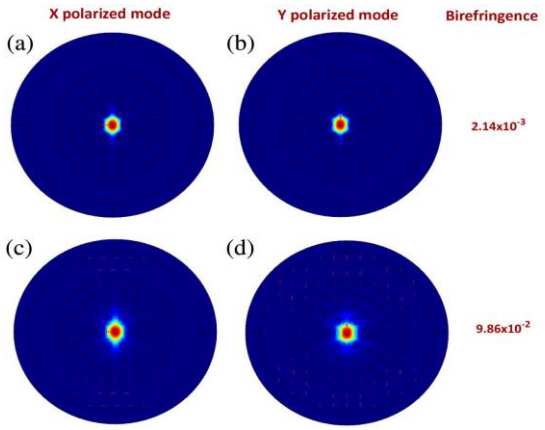

Fig - 4: Electric field distributions of FM for the proposed PQF in the wavelengths of 4.1 μm [(a) and (b)] and 15 μm [(c) and (d)] for X and Y polarized modes.

These results of this sub-section describe that the proposed PM PQF shows the negative dispersion in the lower wavelengths up to 4.2 μm and less positive dispersion regime beyond the wavelengths of 4.4 μm. Thus, this dispersion profile of both the X and Y polarized modes are expected to enhance the continuum broadening for a wide range of wavelengths in MIR.

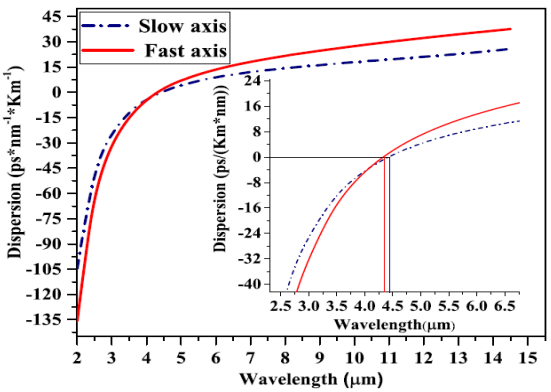

Fig - 5: Changes in dispersion characteristics for the slow and fast axes of the proposed PQF as a function of wavelengths. Inset, changes in dispersion characteristics for a wavelength range of 2 to 6.75 μm for the slow and fast axes.

4. SUPERCONTINNUM GENERATION

Figures. 6 (a) and 6 (b) illustrate the SC broadening along the slow (0°) and fast (90°) axes with a power level of −30 dB for various lengths of the proposed PQF. A pulse of 50 fs with a peak power of 2 kW is polarized at 0° and 90° with respect to the X axis of the proposed PQF. When the input pulse is launched into the fiber for a length, L, of 3 mm, the spectrum of slow and fast axes experiences a strong SPM, because, L = 3 mm > LNL (= 2.16 × 10−3 m and 2.13 × 10−3 m for the slow and fast axes, respectively) and L = 3 mm < LD (=1.2 × 10−2 m and 1.1 × 10−2 m for the slow and fast axes, respectively). At early, SPM dominates in the spectral broadening followed by the soliton fission in which Higher order structures break up into fundamental solitons around the length of 5 mm for both the fast axes (Lf = 4.8 × 10−3 m) and slow (Lf = 5.1 × 10−3 m) . Further, the propagating solitons undergo continuous red shift due to the Raman self-frequency shift for both the axes. Eventually, the spectrum is broadened for the wavelengths from 2 fto 15 μm (~2.9 octaves) for both the axes.

Further, it is noted that the output spectrum phase evolution of the two orthogonally polarized modes are different due to minimal variation in ZDW, nonlinear lengths and γ for both the axes. Nevertheless, it can also generate almost the same spectrum bandwidth with the same input peak power and pulse duration for both the axes. Moreover, the results in Figs. 6 (a) and 6 (b) have confirmed that the SC spectrum broadening does not change beyond 15 μm for the PQF length of 7 mm for both the axes.

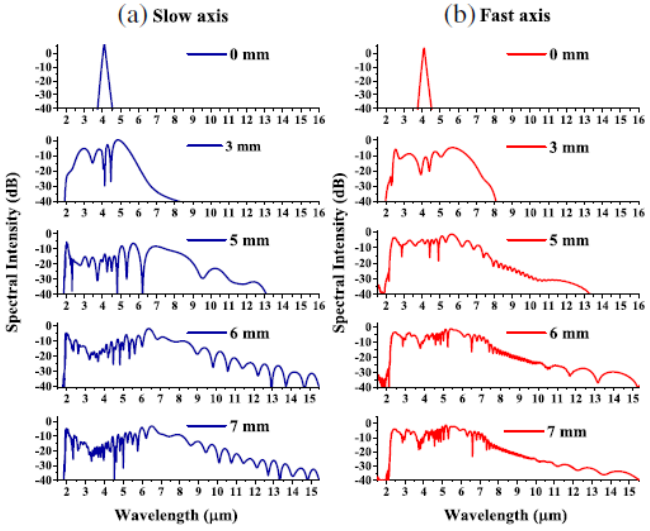

Fig - 6: Numerical demonstration of SC broadening along (a) slow axis (0°) and (b) fast axis (90°) for various lengths of the proposed PQF. The 50 fs input pulse has been launched at the peak power of 2 kW.

Figure 7(a) shows the SC spectrum for both slow and fast axes when the input pulse is polarized at 45° with respect to the principal axis for various propagation lengths. Subsequently, Fig. 7(b) shows the evolution of ellipticity for the corresponding SC spectrum in Fig. 10(a). When a linearly polarized input pulse is launched into the fiber with respect to the principal axis, the specific output SC spectrum gets elliptically polarized and the state of polarization (SOP) can also vary for different spectral components. To evaluate the SOP of spectral components, the parameter ellipticity, ep, is generally used, and the same is estimated as follows.

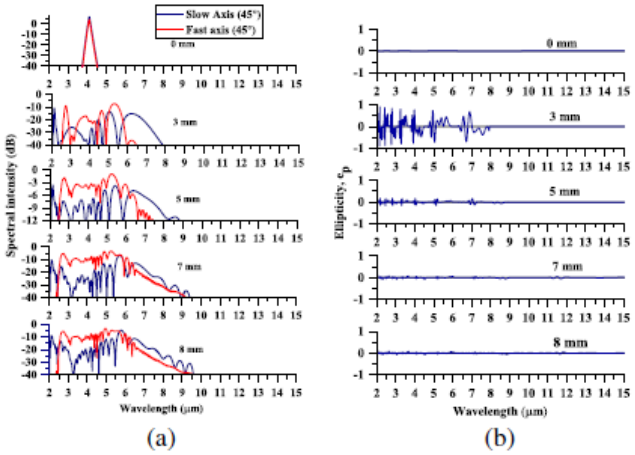

Fig - 7: Evolution of SC along slow (45°) and fast axes (45°) for various propagating lengths of the proposed PQF: (a) spectrum and (b) ellipticity. The 50 fs input pulse has been launched with the peak power of 2 kW.

Initially, in Fig. 7(a), the SOP of SC gets changed due to the variation in the nonlinear polarization rotation which is induced by cross phase modulation (XPM) dependent coupling of two polarized modes. Hence, the nonlinear coupling due to XPM affects the soliton fission process when the PQF length is 3 mm. It is seen in Fig. 7(b) that the ep starts fluctuating randomly over the fiber length of 3 mm. This is due to soliton fission which creates pulses with different polarization states. And, XPM induced coupling also increased up to the length of 3 mm. Therefore, ep has also evolved quite differently for every slice of the spectrum for the PQF length of 3 mm. Further, the XPM induced coupling ceases after the walk-off length of 4.06 mm. Beyond this length, the HOS splits into fundamental soliton with different SOP. Moreover, the fluctuation in the SOP starts to decrease from short wavelengths to longer wavelengths due to the increase of birefringence. Then, ep becomes smaller fluctuation beyond the wavelength of 6.55 μm in the fiber length of 5 mm. Further, in the 7 mm propagation length, the small fluctuations in ep gets minimized due to stable soliton pulses creation in the SC spectrum up to the wavelength of 9.5 μm. Once the fiber length reaches 8 mm, ep becomes very smooth because the SOP of the SC spectrum becomes very stable and does not fluctuate through soliton self-frequency shift. Therefore, the SOP of SC spectrum is preserved at the fiber length of 8 mm. Therefore, we have fixed the length of the proposed PQF as 8 mm for all further studies.

5. CONCLUSIONS

In this paper, we have numerically demonstrated the SC generation in $Ge_{11.5}As_{24}Se_{64.5}$ PM PQF. The proposed PQF is designed with two large air holes near the core which provide a birefringence value in the order of 10^{-4} to 10^{-2} for the wide range of wavelengths from 2 to 15 μm. Further, we exploit the unique property of six-fold symmetric PQF (V number = π for the air-filling ratio of 0.525) that provides the flexibility to increase the cladding air hole diameter beyond the limit for PCF. Therefore, the low CL of 10−7 to 10−1 has been achieved for the wavelengths range from 2 to 15 μm with single mode behavior. Further, the polarization preserving spectrum of SC has broadened from 2 to 15 μm wavelengths in the PQF length of 8 mm when the input pulse is at the pump wavelength of 4.1 μm. The enhanced spectral broadening characteristics of SCG in the proposed PM PQF can be exploited for applications from medical to material processing.

REFERENCES

[1] J. C. Knight, "Photonic crystal fibres," Nature 424, 847–851 (2003).

[2] J. R. Dudley and J. M. Taylor, "Ten years of nonlinear optics in photonic crystal fibre," Nat. Photonics 3, 85–90 (2009).

[3] A. Barh, S. Ghosh, R. Varshney, and B. P. Pal, "Ultra-large mode area microstructured core chalcogenide fiber design for mid-IR beam delivery," Opt. Commun. 311, 129–133 (2013).

[4] J. M. Dudley, G. Genty, and S. Coen, "Supercontinuum generation in photonic crystal fiber," Rev. Mod. Phys. 78, 1135–1184 (2006).

[5] X. Jiang, N. Y. Joly, M. A. Finger, F. Babic, G. K. L. Wong, J. C. Travers, and S. J. Russell, "Deep-ultraviolet to mid-infrared supercontinuum generated in solid-core ZBLAN photonic crystal fibre," Nat. Photonics 9, 133–139 (2014).

[6] R. Cherif, "Highly nonlinear As2Se3-based chalcogenide photonic crystal fiber for midinfrared supercontinuum generation," Opt. Eng.49, 095002 (2010).

[7] A. Bétourné, A. Kudlinski, G. Bouwmans, O. Vanvincq, A. Mussot, and Y. Quiquempois, "Control of supercontinuum generation and soliton self-frequency shift in solid-core photonic bandgap fibers," Opt. Lett. 34, 3083–3085 (2009).

[8] B. Ung and M. Skorobogatiy, "Chalcogenide microporous fibers for linear and nonlinear applications in the mid-infrared," Opt. Express 18, 8647–8659 (2010).

[9] U. Møller, Y. Yu, I. Kubat, C. R. Petersen, X. Gai, L. Brilland, D. Méchin, C. Caillaud, J. Troles, B. Luther-Davies, and O. Bang, "Multi-milliwatt mid-infrared supercontinuum generation in a suspended core chalcogenide fiber," Opt. Express 23, 3282–3291 (2015).

[10] I. Kubat, C. S. Agger, U. Møller, A. B. Seddon, Z. Tang, S. Sujecki, T. M. Benson, D. Furniss, S. Lamrini, K. Scholle, P. Fuhrberg, B. Napier, M. Farries, J. Ward, P. M. Moselund, and O. Bang, "Mid-infrared supercontinuum generation to 12.5 μm in large NA chalcogenide step-index fibres pumped at 4.5 μm," Opt. Express 22, 19169–19182 (2014).

[11] T. Cheng, Y. Kanou, X. Xue, D. Deng, M. Matsumoto, T. Misumi, T. Suzuki, and Y. Ohishi, "Mid-infrared supercontinuum generation in a novel AsSe2–As2S5 hybrid microstructured optical fiber," Opt. Express 22, 23019–23025 (2014).

[12] Z. Tang, V. S. Shiryaev, D. Furniss, L. Sojka, S. Sujecki, T. M. Benson, A. B. Seddon, and M. F. Churbanov, "Low loss Ge-As-Se chalcogenide glass fiber, fabricated using extruded preform, for mid-infrared photonics," Opt. Mater. Express 5, 1722–1737 (2015).

[13] Y. Yu, B. Zhang, X. Gai, C. Zhai, S. Qi, W. Guo, Z. Yang, R. Wang, D.-Y. Choi, S. Madden, and B. Luther-Davies, "1.8–10 μm midinfrared supercontinuum generated in a step-index chalcogenide fiber using low peak pump power," Opt. Lett. 40, 1081–1084 (2015).

[14] C. R. Petersen, U. Møller, I. Kubat, B. Zhou, S. Dupont, J. Ramsay, T. Benson, S. Sujecki, N. Abdel-Moneim, Z. Tang, D. Furniss, A. Seddon, and O. Bang, "Mid-infrared supercontinuum covering the 1.4–13.3 μm molecular fingerprint region using ultra-high NA chalcogenide step-index fibre," Nat. Photonics 8, 830–834 (2014).

[15] T. Cheng, K. Nagasaka, T. H. Tuan, X. Xue, M. Matsumoto, H. Tezuka, T. Suzuki, and Y. Ohishi, "Mid-infrared supercontinuum generation spanning 2.0 to 15.1 μm in a chalcogenide step-index fiber," Opt. Lett. 41, 2117–2120 (2016).

[16] M. R. Karim, B. M. A. Rahman, Y. O. Azabi, A. Agrawal, and G. P. Agrawal, "Ultrabroadband mid-infrared supercontinuum generation through dispersion engineering of chalcogenide microstructured fibers," J. Opt. Soc. Am. B 32, 2343–2351 (2015).

[17] B. Luther-Davies, Amorphous Chalcogenides (Pan Stanford Publishing, 2014).

[18] X. Su, R. Wang, B. Luther-Davies, and L. Wang, "The dependence of photosensitivity on composition for thin films of GexAySe1−x−y chalcogenide glasses," Appl. Phys. A 113, 575–581 (2013).

[19] S. Kim, C.-S. Kee, and J. Lee, "Novel optical properties of six-fold symmetric photonic quasicrystal fibers," Opt. Express 15, 13221– 13226 (2007).